a Identity (%)

Zebrafish	100													
Xenopus	55.32	100												
Chicken	53.93	72.02	100											
Mouse	55.03	71.6	78.12	100										
Rat	54.96	71.39	78.19	97.12	100									
Guinea pig	54.06	71.17	78.95	92.06	92.58	100								
Pig	52.74	69.27	76.43	89.57	89.92	91.27	100							
Cow	54.71	71.9	79.14	91.78	92.05	92	93.29	100						
Rabbit	55.49	71.83	79.14	92.46	92.94	92.51	91.68	93.77	100					
Macaque	55.21	72.07	79.32	92.79	93.14	93.16	92.37	94.04	95.34	100				
Gorilla	53.16	71.14	79.53	92.3	92.53	92.83	93.97	93.29	94.65	98.79	100			
Orangutan	54.36	71.92	80.07	92.58	92.87	92.95	93.36	93.76	95.01	99.05	99.25	100		
Human	55.17	72.16	79.33	92.66	93.07	92.87	91.95	93.77	95.14	99.04	99.25	99.34	100	
Chimpanzee	55.17	72.3	79.55	92.8	93.21	93.02	92.16	93.97	95.34	99.18	99.47	99.56	99.73	100
	Zebrafish	Xenopus	Chicken	Mouse	Rat	Guinea pig	Pig	Cow	Rabbit	Macaque	Gorilla	Orangutan	Human	Chimpanzee

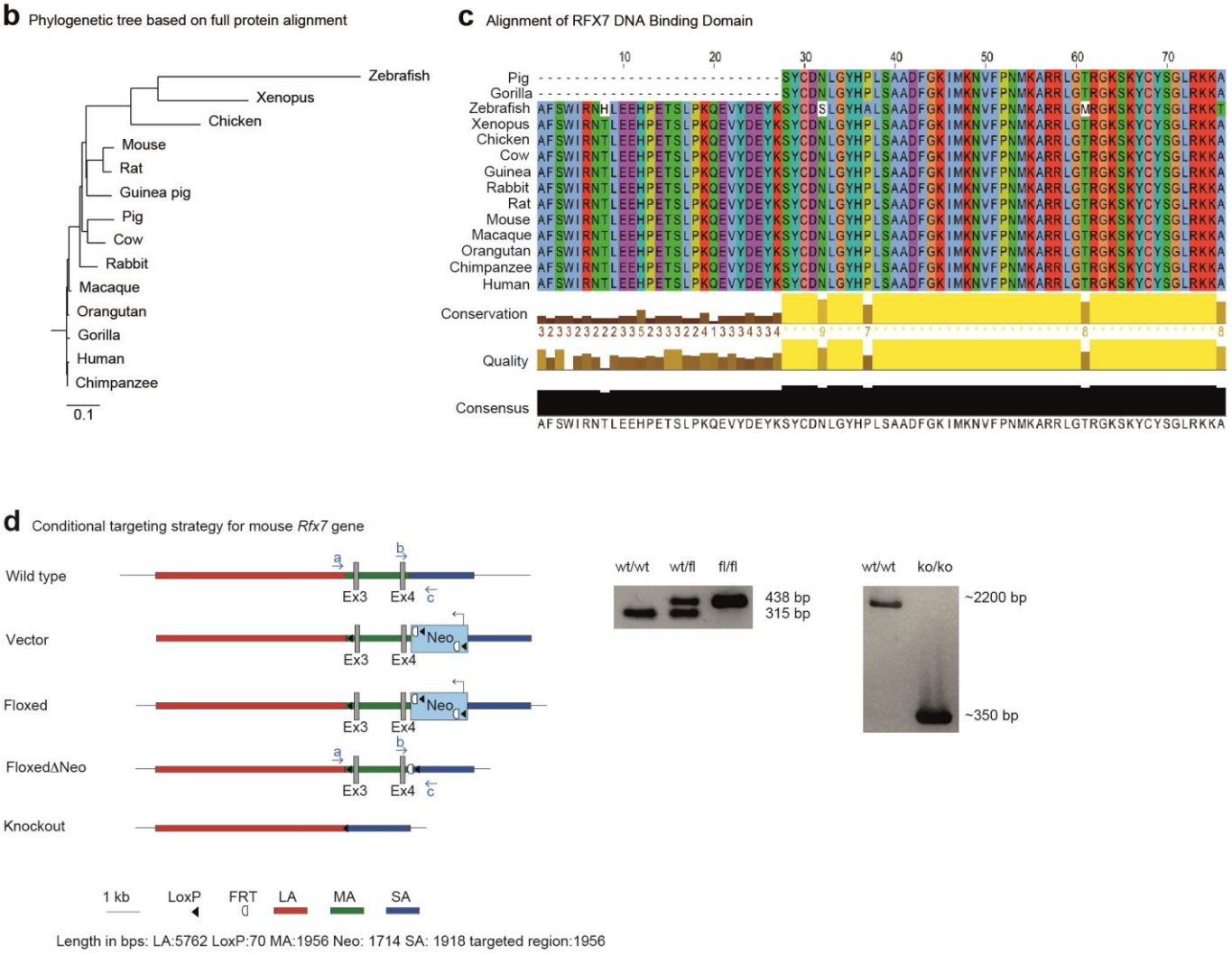

Supplementary Figure 1

Rfx7 phylogeny and conditional-knockout strategy.

(a) Percent identity matrix of full RFX7 protein sequences generated with Clustal 2.1. (b) Phylogenetic tree based on full protein alignment (Neighbor-joining tree without distance corrections, Clustal 2.1); the bar line (distance scale) indicates the percentage of variation among species, i.e. 0.1 represent 10% difference between two sequences. (c) Alignment of RFX7 DNA Binding Domain for the indicated species (JalView). The

compared protein sequences correspond to the following species: Human, *Homo sapiens*; Chimpanzee, *Pan troglodytes*; Gorilla, *Gorilla gorilla*; Macaque, *Macaca mulatta*; Orangutan, *Pongo pygmaeus*; Mouse, *Mus musculus*; Rat, *Rattus norvegicus*; Rabbit, *Oryctolagus cuniculus*; Guinea pig, *Cavia porcellus*; Pig, *Sus scrofa*; Cow, *Bos taurus*; Chicken, *Gallus gallus*; Xenopus, *Xenopus tropicalis*; Zebrafish, *Danio rerio*. (d) Scheme showing the targeting strategy for the conditional knockout of the murine *Rfx7* gene. The vector was designed such as the 5' loxP site is inserted upstream of exon 3 and the target region is 1.96 kb including exons 3-4. The loxP/FRT flanked Neo cassette is inserted downstream of exon 4. The selection cassette (Neo) was excised by crossing floxed mice with FLP deleter line. The two loxP sites shown allow Cre-mediated deletion of exons 3 (Ex 3) and 4 (Ex 4). PCR primers b/c discriminate wild type (wt) and floxed (fl) *Rfx7* alleles and primers a/c wild type and knockout (ko) *Rfx7* alleles. Arrows on diagram indicate PCR primer positions. PCR products obtained for each genotype are shown. LA: long arm, MA: middle arm, SA: short arm, FRT: flippase recognition target, Neo: neomycine cassette.

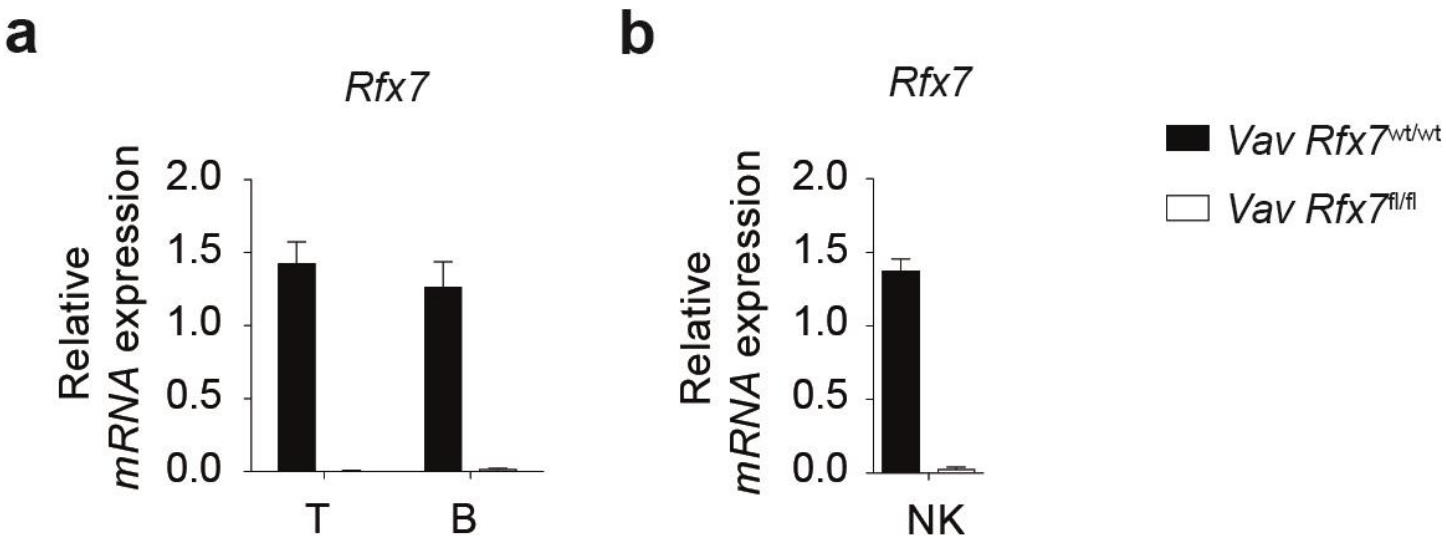

Supplementary Figure 2

Rfx7 deletion is highly efficient in immune cells.

(a,b) Quantitative RT-PCR (qRT-PCR) data (relative to *Polr2a*) showing *Rfx7* transcript abundance in MACS-sorted T and B cells (a), and in FACS-sorted NK lymphocytes (b) from *Vav Rfx7*$^{fl/fl}$ and *Rfx7*$^{fl/fl}$ mice. Results represent mean ± SD of technical replicates (n=3) and are representative of at least two experiments (a,b).

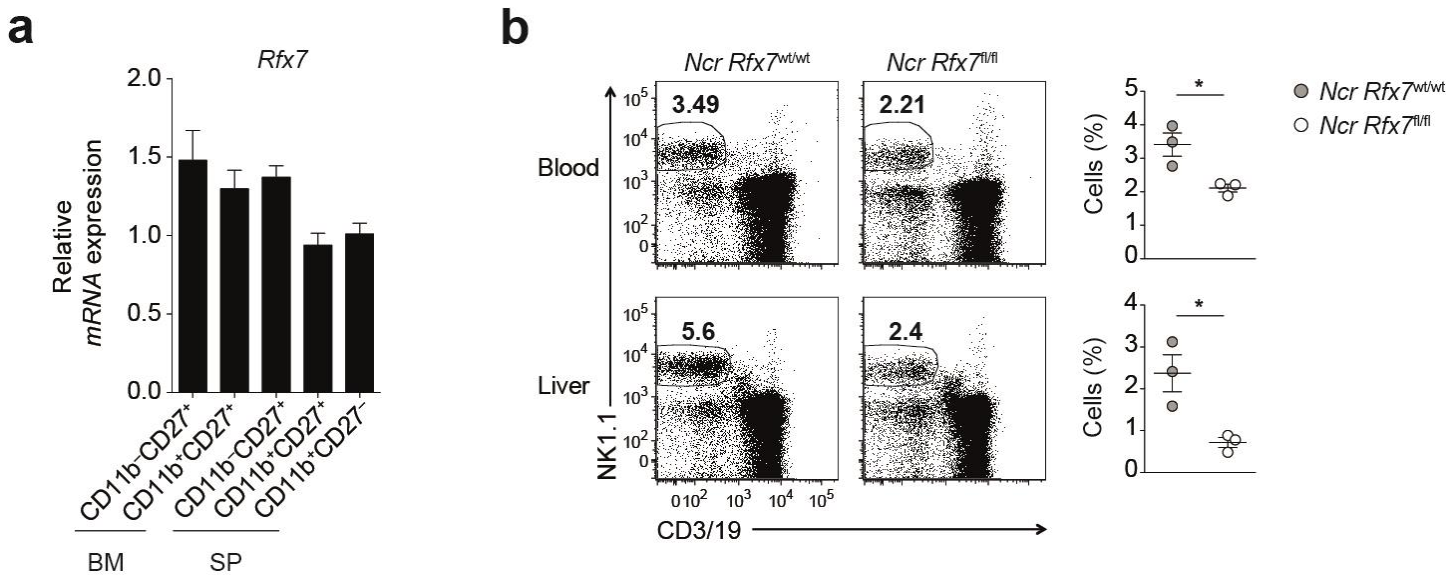

Supplementary Figure 3

Rfx7 deficiency affects NK cells in various tissues.

(a) The abundance of *Rfx7* mRNA was determined by qRT-PCR in the indicated subsets of sorted NK cells from BM or spleen (SP) of wild type mice (relative to *Polr2a*). (b) A representative flow cytometric plot of NK cells (gated as $NK1.1^{+}CD3^{-}CD19^{-}$) in the blood and liver of *Ncr Rfx7*$^{wt/wt}$, and *Ncr Rfx7*$^{fl/fl}$ mice is shown (gated on $CD45^{+}$ lymphocytes). Results represent the mean ± SD of n=3 technical replicates (a) or the mean ± SEM of n=3 mice/group (b) and are representative of at least two independent experiments (a,b). (b) Statistical comparison between the experimental condition lacking Rfx7 and control were performed; *$p \leq 0.05$; Student's t-test.

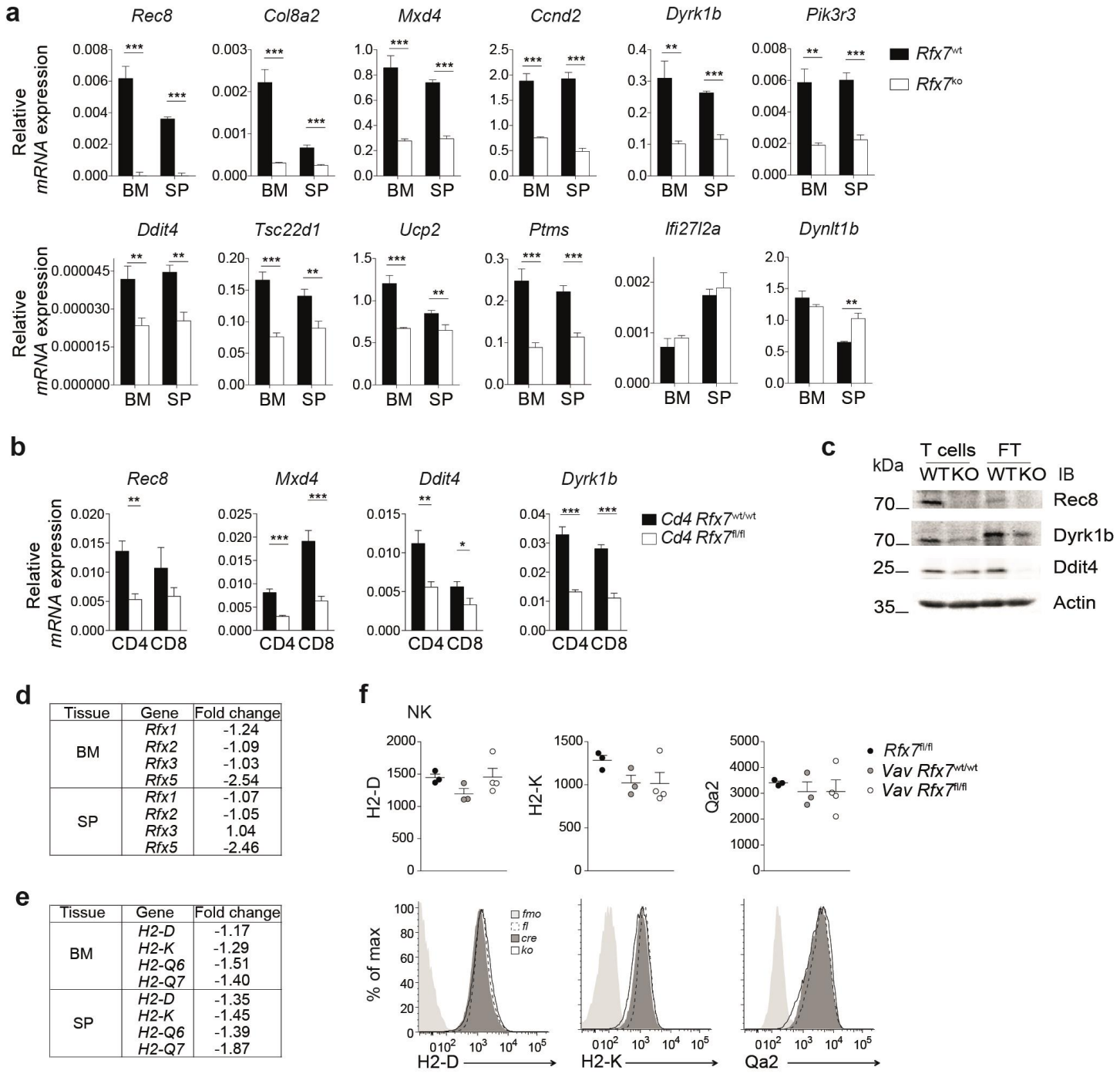

Supplementary Figure 4

Validation of genes intrinsically regulated by Rfx7.

(a) Control and Rfx7-deficient NK cells were isolated from BM (sorted as CD122$^+$ NK1.1$^+$) and spleen (sorted as Ncr1$^+$ and NK1.1$^+$) from a pool of nine *Vav Rfx7* $^{wt/wt}$:*Vav Rfx7* $^{fl/fl}$ mixed BM chimeras. Transcript abundance of 12 genes, selected based on the RNA-sequencing results, was determined by qRT-PCR (relative to *Polr2a*). (b) MACS-sorted CD4$^+$ and CD8$^+$ T cells from spleens of *Cd4 Rfx7*$^{wt/wt}$ and *Cd4 Rfx7*$^{fl/fl}$ mice were tested for mRNA levels of the indicated genes by qRT-PCR (relative to *Polr2a*). (c) Expression of the indicated proteins

in MACS-enriched T cells and T cell-depleted fractions (flow through, FT) from splenocytes of *Vav Rfx7*$^{wt/wt}$ or *Vav Rfx7*$^{fl/fl}$ mice was determined by immunoblot analysis. Actin was used as loading control. (d,e) Table illustrating the fold difference (KO:WT) detected in the RNA-sequencing for *Rfx* genes (d) or the indicated MHC-related genes (e) in BM or spleen NK cells. f) Graphs depict the geometric MFI of surface H2-D, H2-K, and Qa2 as detected on NK cells of the indicated genotypes and a representative histogram thereof. Results depict mean ± SD of n=3 technical replicates per genotype/organ (a) or the mean ± SEM of n=3 (*Cd4 Rfx7*$^{wt/wt}$) and n=5 (*Cd4 Rfx7*$^{fl/fl}$) mice (b) and of n=3 (*Rfx7*$^{fl/fl}$), n=3 (*Vav Rfx7*$^{wt/wt}$) and n=4 (*Vav Rfx7*$^{fl/fl}$) mice (f). Results are representative of at least two independent experiments (a,b,c,f). (a,b,f) Statistical comparison between the experimental condition lacking Rfx7 and controls were performed; *$p \leq 0.05$, **$p \leq 0.01$, ***$p \leq 0.001$; Student's t-test.

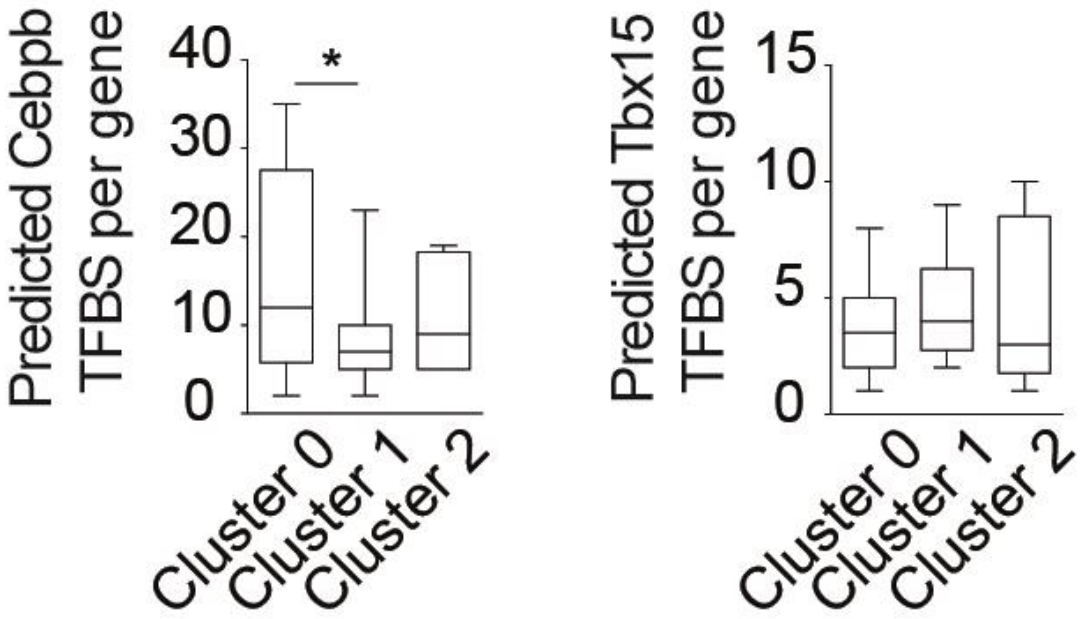

Supplementary Figure 5

Analyses of Rfx7-target genes in silico.

(a) *In Silico* analysis of promoter sequences (-700; +300) of differentially expressed genes from cluster 1 (downregulated genes), cluster 2 (upregulated genes), and cluster 0 (non-modulated genes, serving as control group) was performed with JASPAR tool for the presence of putative transcription factor binding sites (TFBS) for CCAAT/enhancer binding protein beta (Cebpb) and T-box 15 (Tbx15). The box and whisker plots depict the number of putative TFBS identified with a relative profile score threshold of 0.8. Significance was determined using one-tail Mann-Whitney tests; *$p \leq 0.05$.

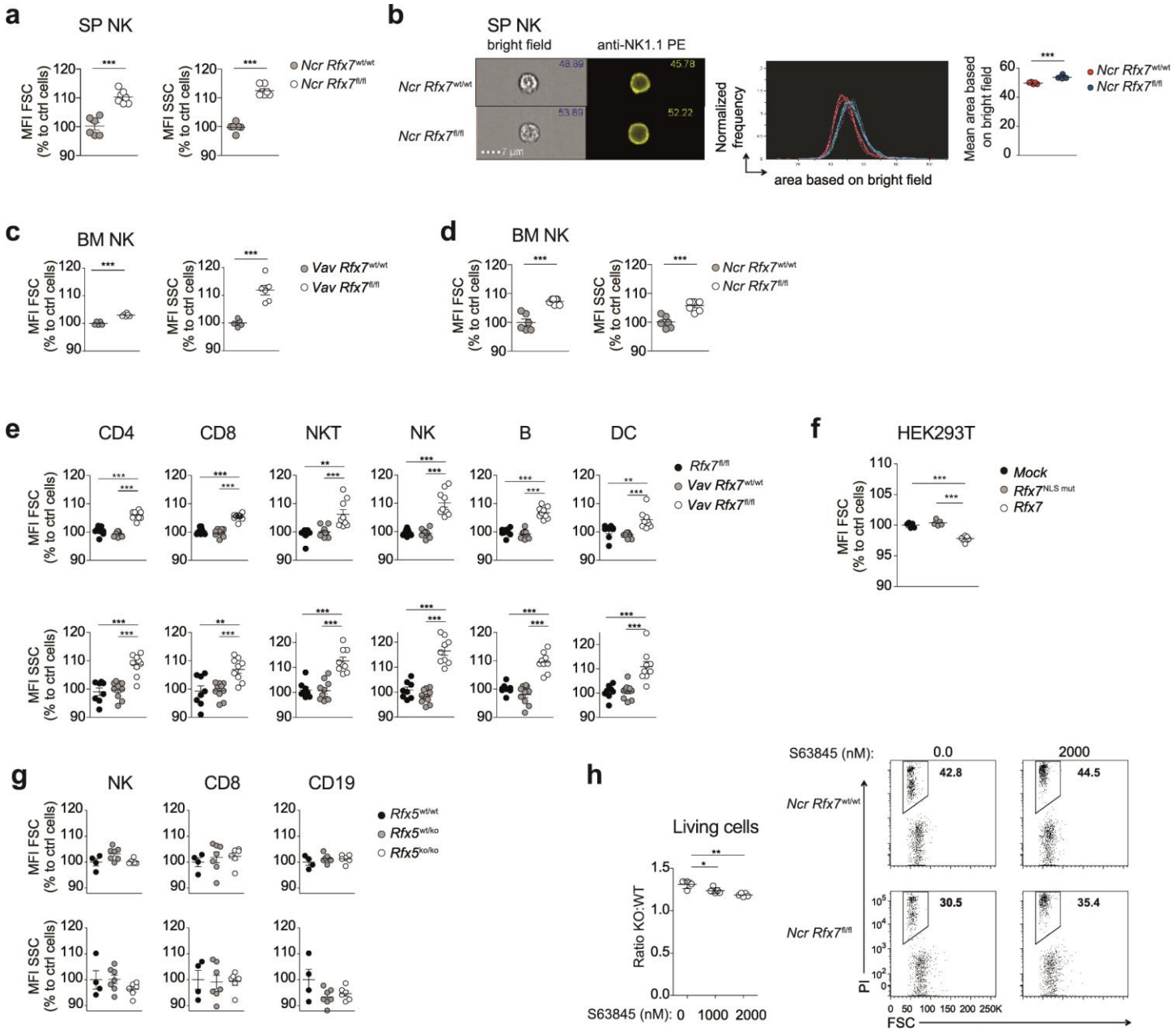

Supplementary Figure 6

Rfx7-dependent regulation of size and granularity.

(a) Quantification of forward scatter (FSC) and side scatter (SSC) for splenic NK cells (gated as NK1.1$^+$ CD3/19$^-$) from *Ncr Rfx7*$^{wt/wt}$ (set as 100%) and *Ncr Rfx7*$^{fl/fl}$ mice. (b) A representative ImageStream picture of NK cells (bright field or anti-NK1.1 staining) from *Ncr Rfx7*$^{wt/wt}$ and *Ncr Rfx7*$^{fl/fl}$. Histogram illustrates the surface area based on the bright field of 30'000 to 100'000 cells per mouse and genotype and the graph a quantification thereof (each line colored in hues of red or blue represents one mouse, *Ncr Rfx7*$^{wt/wt}$ and *Ncr Rfx7*$^{fl/fl}$, respectively). (c,d) FSC and SSC for BM NK cells (gated as CD122$^+$ CD3/19$^-$) are shown for *Vav Rfx7*$^{wt/wt}$, and *Vav Rfx7*$^{fl/fl}$ mice (c) and for *Ncr Rfx7*$^{wt/wt}$ and *Ncr Rfx7*$^{fl/fl}$ mice (d). (e) Quantification of FSC and SSC for splenic CD4$^+$ T cells (gated as CD3$^+$CD4$^+$), CD8$^+$ T cells (gated as CD3$^+$CD8$^+$), NKT cells (gated as NK1.1$^+$CD3$^+$), NK cells (gated as NK1.1$^+$CD3$^-$), B cells (gated as CD19$^+$), and conventional dendritic cells

(DC; gated as $CD11c^{hi}CD11b^{int–hi}$) from the indicated mice. (f) HEK293T cells were co-transfected with WT, NLS-mutant (m658 & 674) *Rfx7*, or empty (mock) and GFP-encoding vectors. After 48 hours, FSC was analyzed on the GFP^+ cells, with the FSC of mock-transfected cells set at 100. (g) Quantification of FSC and SSC for splenic NK cells, $CD8^+$ T cells, and B cells from $Rfx5^{+/+}$, $Rfx5^{+/–}$, and $Rfx5^{–/–}$ mice. (h) The graph depicts ratios of Rfx7-deficient to control living NK cells (congenically marked) co-cultured in the presence of high IL-15 and S63845 (Mcl-1 inhibitor; Cayman Chemical) for three days (normalized to initial mix). Flow cytometry plots illustrate dead cell percentage. Results represent the mean ± SEM of n=6 (*Ncr* $Rfx7^{wt/wt}$) and n=7 (*Ncr* $Rfx7^{fl/fl}$) (a,d), n=5 (*Ncr* $Rfx7^{wt/wt}$) and n=8 (*Ncr* $Rfx7^{fl/fl}$) (b), n=5 (*Vav* $Rfx7^{wt/wt}$) and n=6 (*Vav* $Rfx7^{fl/fl}$) (c), n=8 ($Rfx7^{fl/fl}$), n=10 (*Vav* $Rfx7^{wt/wt}$), and n=9 (*Vav* $Rfx7^{fl/fl}$) (e), n=4 ($Rfx5^{+/+}$), n=7 ($Rfx5^{+/–}$), and n=6 ($Rfx5^{–/–}$) mice (g) or mean ± SD of n=4-5 technical replicates per condition (f,h) and are representative of at least two independent experiments (a-f) and a pool of two independent experiments (g,h). Statistical comparison between the experimental condition and controls were performed; ***$p \leq 0.001$; Student's t-test (a-g).

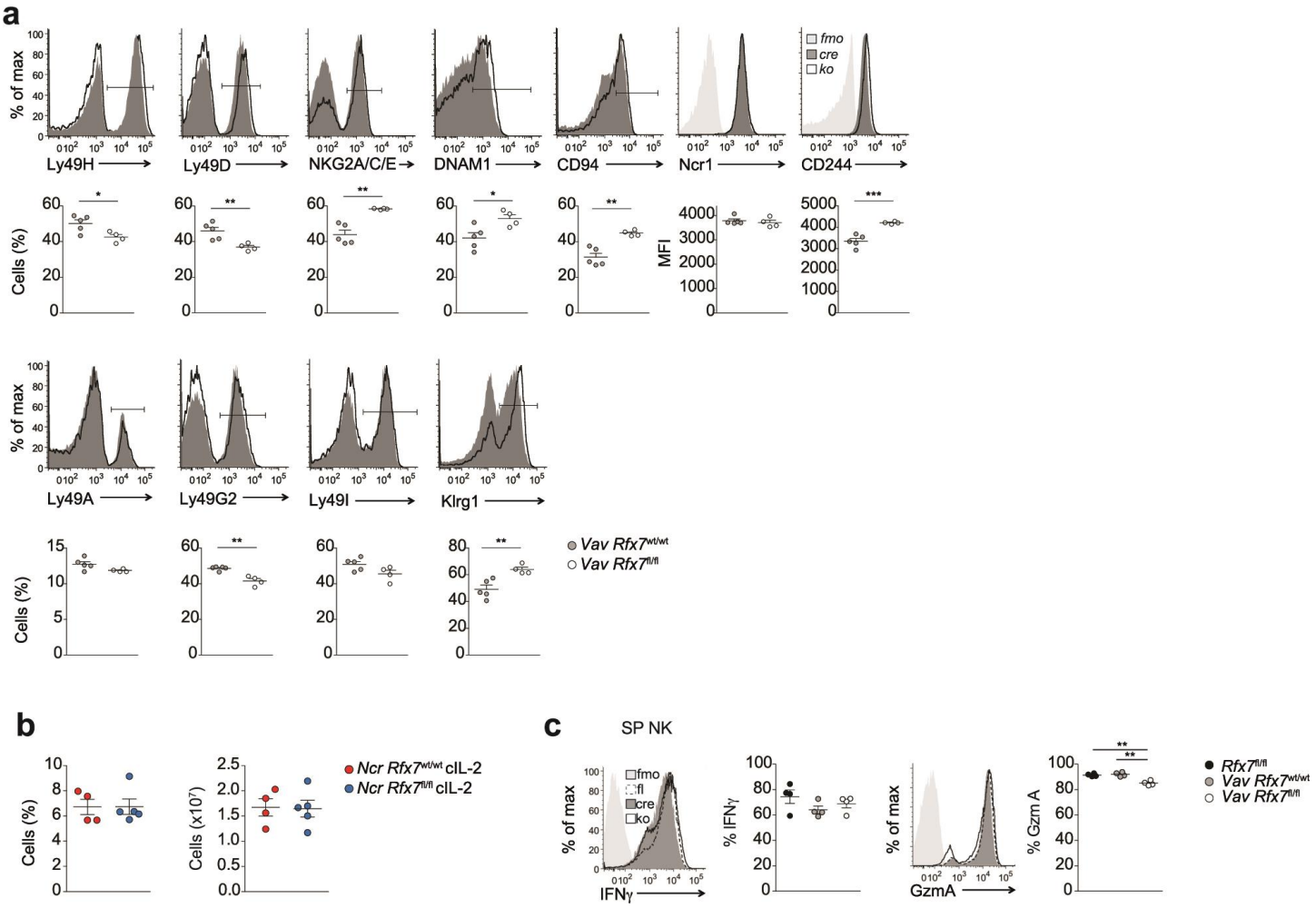

Supplementary Figure 7

Rfx7-deleted NK cells present only moderate alterations in functional features.

(a) Expression analysis of the indicated receptors on splenic NK cells (NK1.1^{+}CD3^{-}CD19^{-}) from *Vav Rfx7*$^{wt/wt}$, and *Vav Rfx7*$^{fl/fl}$ mice is depicted as percentage of positive population (for biphasic expression) or geometric MFI. (b) Percentages and numbers of NK cells (gated as NK1.1^{+} and CD3/19^{-}) in the spleen of *Ncr Rfx7*$^{fl/fl}$ and *Ncr Rfx7*$^{wt/wt}$ mice treated with IL-2 complexes (cIL-2) for four days and used for *B2m*$^{-/-}$ splenocyte rejection on day 5 (presented in Fig. 8c) are depicted. (c) A representative flow cytometric plot and a quantification of IFNγ and granzyme A production by splenic NK cells of *Rfx7*$^{fl/fl}$, *Vav Rfx7*$^{wt/wt}$, and *Vav Rfx7*$^{fl/fl}$ mice are shown. Results represent the mean ± SEM of n=5 (*Vav Rfx7*$^{wt/wt}$) and n=4 (*Vav Rfx7*$^{fl/fl}$) (a) or n=4 (*Ncr Rfx7*$^{wt/wt}$) and n=5 (*Ncr Rfx7*$^{fl/fl}$) mice (b), or n=4 (c) and are representative of at least two independent experiments (a-c). Statistical comparison between the experimental condition lacking Rfx7 and controls were performed; *$p \leq 0.05$, **$p \leq 0.01$, ***$p \leq 0.001$; Student's t-test.

Table 1a

TRANSCRIPTION FACTORS INVOLVED IN NK CELL DEVELOPMENT

Gene symbol	Fold change BM	Fold change SP
Tbet/Tbx21	-1.21	-1.22
Prdm1/Blimp	-1.18	1.22
Gata3	-1.16	1.03
Zeb2	-1.13	1.14
Elf4/MEF	-1.11	1.23
Stat4	-1.10	1.18
Mcm4	-1.09	1.14
Tox	-1.08	1.19
Eomes	-1.08	1.04
Stat5b	-1.07	1.08
Irf2	-1.04	1.10
Ets1	-1.02	1.42
Ikzf1	1.01	1.15
Notch1	1.02	1.01
Tcf3/E2A	1.03	1.04
E4bp4/Nfil3	1.04	-1.18
Id2	1.08	1.07
Spi1/PU.1	1.70	-1.32

Table 1b

CYTOKINE RECEPTORS AND SIGNALING MOLECULES INVOLVED IN NK CELL DEVELOPMENT

Gene symbol	Fold change BM	Fold change SP
Il2ra	-1.41	1.85
Il12rb2	-1.32	1.08
Il2rg	-1.13	-1.03
IL18rap	-1.10	1.04
IL15ra	1.09	1.02
Il2rb/Cd122	-1.08	1.02
Il12rb1	-1.08	-1.12
Il7r	-1.08	2.67
Ifnar1	-1.06	1.05
IL18r1	-1.02	1.06
Ifnar2	-1.02	1.01

!

Table 2

CYTOTOXIC MEDIATORS

Gene symbol	Fold change BM	Fold change SP
Gzmc	-2.23	-1.38
Gzmb	-2.03	-1.65
Gzma	-1.32	-1.40
Tnfsf6/Fasl	-1.11	-1.15
Ifng	-1.06	1.01
Prf1	-1.06	-1.15
Tnfsf10/Trail	1.14	1.83
Gzmm	1.32	1.04
Gzmk	1.58	1.82
Tnf	1.82	1.73